Heliyon 8 (2022) e09609

Contents lists available at ScienceDirect

Heliyon

journal homepage: www.cell.com/heliyon

Research article

Modification of epoxy binder with multi walled carbon nanotubes in hybrid fiber systems used for retrofitting of concrete structures: evaluation of strength characteristics

Lakshmi Joseph [a], P. Sarath Kumar [b,c], B.D.S. Deeraj [d], K. Joseph [d], Karingamanna Jayanarayanan [b,c,**], K.M. Mini [a,*]

[a] Department of Civil Engineering, Amrita School of Engineering, Amrita Vishwa Vidyapeetham, Coimbatore, India
[b] Department of Chemical Engineering and Materials Science, Amrita School of Engineering, Amrita Vishwa Vidyapeetham, Coimbatore 641112, India
[c] Centre of Excellence in Advanced Materials and Green Technologies (CoE-AMGT), Amrita School of Engineering, Amrita Vishwa Vidyapeetham, Coimbatore 641112, India
[d] Department of Chemistry, Indian Institute of Space Science and Technology, Thiruvananthapuram, Kerala, India

ARTICLE INFO

Keywords:
Epoxy
MWCNT
Hybrid fiber
Confinement
Retrofitting
Ductility index
Energy absorption

ABSTRACT

The rapid development in infrastructural facilities necessitates an efficient approach for the repair and retrofitting of concrete structures and, confinement method using fiber reinforced polymer is a promising one. The commonly used carbon and glass fibers for confinement poses environmental and performance issues. The present study addresses these two major aspects by considering natural fibers along with modification of epoxy binder to impart ductile behavior ie., to investigate the effectiveness of multiwalled carbon nanotubes (MWCNT) incorporated synthetic and natural fiber reinforced polymer (FRP) systems as the external confinement. MWCNT is incorporated in 0.5–1.5wt.% in epoxy nano and epoxy multiscale and there is significant enhancement in tensile and fracture properties of the composites up to 1wt.%, beyond which it declined due to agglomeration. Various strength tests were performed with sisal, basalt, carbon and hybrid sisal-basalt FRP systems with different FRP layer thickness on plain concrete cylinders. From the test results it is outlined that external confinement with MWCNT incorporated FRP improved the axial load-carrying capacity, energy absorption and ductility of concrete with respect to that of control specimens. Compared with unconfined specimens, those strengthened with MWCNT modified hybrid FRP wraps containing sisal and basalt fibers recorded increments of 114% and 87% in their load-carrying capacity and energy absorption, due to the intrinsic rigidity of hybrid fibers and epoxy modification. Furthermore, the outcomes indicate that MWCNT incorporated hybrid sisal-basalt FRP confined specimens exhibited superior properties and the low strength of natural FRP confinement compared to artificial FRP can be improved by epoxy modification. The outer jacketing resisted abrupt and catastrophic failure to a great extent.

1. Introduction

The repair and strengthening of damaged structures are of immense importance in infrastructure development. The damaged and structurally inadequate buildings should be rebuilt or strengthened to maintain safety requirements and structural integrity. Due to the environmental impacts and high cost, demolition and rebuilding options of the existing structures may not be a viable option. In order to ensure the serviceability and safety of structures there is a pressing need for development of strengthening and retrofitting techniques [1]. Off late, fiber reinforced polymer (FRP) composites have been developed as a possible material for strengthening and retrofitting. The ease of installation, corrosion resistance, high strength to weight ratio and improved tensile strength are the most appealing attributes of FRPs which further qualifies those as materials of immense relevance in structural rehabilitation. The concrete confinement not only improved the load bearing capacity but also the energy absorption and ductility of the concrete [2, 3].

* Corresponding author.
** Corresponding author.
E-mail addresses: kj_narayanan@cb.amrita.edu (K. Jayanarayanan), k_mini@cb.amrita.edu (K.M. Mini).

https://doi.org/10.1016/j.heliyon.2022.e09609
Received 9 February 2022; Received in revised form 11 April 2022; Accepted 26 May 2022

For concrete retrofitting, natural fibers like coir, jute, sisal and flax etc. were used since they have low density, low cost, moderate tensile and flexural properties with respect to the synthetic fiber counterparts. The natural fibers have an extraordinary capability in the retrofitting of concrete structures [4, 5]. The load-bearing capacity and energy absorption characteristics could be improved by jute and sisal fiber confinement [6, 7]. Further studies [8, 9, 10] have shown that hybridization of natural and synthetic fibers helped in providing an improved solution [11, 12]. It was also noticed that there is increment in strain, energy dissipation capacities and improved strength for various hybrid configurations [13, 14]. Apart from FRP application fabric reinforcements are widely used in fabric reinforced cementitious mortar which is a composite made up of a fiber mesh (or grid) bounded on a structural member by means of an inorganic matrix [15]. In fact, the high-strength of the fabric material and the thick matrix layers combined together offers a significant thermal-resistance [16, 17].

In FRP composites, the thermoset polymer epoxy resin is a widely used matrix material. High strength to weight ratio, specific stiffness, chemical compatibility, and strength makes it appropriate for such applications [18, 19]. Under exposure to severe environmental conditions for greater periods of time, epoxy tends to degrade and results in deterioration of various mechanical properties. Into the traditional fiber reinforced polymer composites when carbon nanotubes (CNTs) were incorporated there would be significant improvement in their properties. High specific surface area offered by CNTs serve as a reason for better stress transfer and filler–polymer interface interaction [20, 21]. However, at higher concentrations, Van der Waals forces between the individual nanotubes result in agglomeration and CNT bundling [22]. For uniform dispersion of nanotubes in polymer resins either sonication or high shear mixing can be employed [23]. There is improved interfacial interaction between epoxy and CNT due to CNT surface functionalization and further helps in the nanofiller dispersion into the matrix [24]. Kumar P S et al. [25, 26] reported that significant improvement was observed on MWCNT addition in fracture and tensile properties of nano and multiscale composites and beyond the optimum weight percentage there is a decrease in the properties owing to MWCNT agglomerations.

The axial behavior of circular and square columns confined with sprayed fiber-reinforced polymer (SFRP) composites was studied by Hussain et al. [27] and reported that the SFRP composite confinement effect on circular columns was more prominent than square columns and also the increase in layers improved the compressive strength and deformability at particular corner radius in case of square columns [28]. Studies on the strengthening of square shaped columns using the high-strength steel-rod collars revealed that it enhances the confinement effect around the column perimeter and high-strength steel-rod collars are effective in shear critical columns. These strengthened specimens exhibit a stable hysteretic behavior, high energy dissipation and greater ductility when compared with unconfined specimens [29, 30]. Pimanmas et al. [31] studied the confinement offered by sisal FRP wrapping and compared the ultimate axial strength and ductility between square and circular columns and reported a considerable enhancement in axial compressive strength and strain in circular columns. Thus, concluded that natural fibers can also be considered as a suitable alternative in FRP retrofitting in spite of its low strength and durability concerns.

From the literature survey it is much evident that an in-depth analysis of nano incorporated epoxy-based hybrid FRP composite as a confinement for concrete strengthening and retrofitting applications have not been explored much. The study aims to analyze the performance and impact of MWCNT incorporated epoxy-based hybrid FRP composites with different layers of hybrid sisal and basalt fiber systems as a jacketing material for unconfined concrete columns subjected to uniaxial loading. Ultimate strength, energy absorption, failure modes, ductility, and stress-strain response are also studied to analyze the performance of confinement. The various test parameters considered are percentage variation of MWCNT in epoxy matrix, type of FRP composites and the number of hybrid composite layers. Experimental results are expected to reveal the feasibility of MWCNT incorporated hybrid FRP composite systems for concrete jacketing in structural applications.

2. Materials and methods

2.1. Materials

2.1.1. Concrete

Grade 53 ordinary Portland cement was used for the preparation of concrete specimens conforming to IS 12269-2013 [32]. The specific gravity of cement was calculated as 3.16 using Le Chatelier flask. Clean river sand of zone III with a fineness modulus of 2.82 and specific gravity of 2.64 was taken as fine aggregates. The bulk density and specific gravity for the coarse aggregate was obtained as 1.51 kg/l and 2.65 with maximum size as 20 mm. A target strength of 25MPa was fixed for all the concrete specimens. The mix proportion of weight of cement: fine aggregate: coarse aggregate was 1:1.5:2.58 with 0.45 water cement ratio as per IS 10262-2009 [33].

2.1.2. CNT modified epoxy

A high-performance two-part epoxy resin was utilized in this experiment. It comprises resin (Part A) and hardener (Part B). They were blended in a mix proportion of 100:15 by weight as recommended by the supplier. The MWCNT modified carboxylic acid (–COOH) with 97% nanotube purity, average length 2–10 microns, outer diameter 5–20 nm and specific surface area 250–270 m^2/g supplied by Platonic Nanotech Private Limited, Jharkhand, India was selected as the nanofiller to improve the adhesion properties of the epoxy along with strength enhancement of the final composites.

2.1.3. Fibers

Sisal and basalt fiber in the form of bidirectional woven plain fabric was supplied by Go green Products, Tamil Nadu. The thickness of fabric layer varied from 0.8 to 1mm. The density of basalt fiber of 380 GSM is 2630 kg/m^3 while density of sisal fiber with 300 GSM is 1580 kg/m^3 as provided by the manufacturer. Plain carbon fiber fabric with 200 GSM, density 1380 kg/m^3 and thickness 0.45 mm was adopted for the study. Sisal fibers were subjected to alkaline treatment by completely immersing them in NaOH solution and drying at room temperature for 72 h [34]. After treatment there is an improvement in surface roughness which further results in improved mechanical interlocking.

2.2. FRP composite preparation

For each composition an estimated amount of MWCNT was uniformly dispersed within the epoxy resin for a period of 30 min using an ultrasonic probe sonicator at 20 kHz frequency. In most of the previous studies [25, 26, 35] the optimum content of CNT was obtained at around 1 wt % and thus Epoxy-MWCNT nanocomposites with nanofiller content 0.5wt. %, 1wt. % and 1.5wt. % were prepared. These composites were then cured at room temperature for a period of 72 h, and assessed for different properties. A two-step method was adopted for composite laminate preparation. The epoxy-MWCNT mixture preparation was the initial step and in the subsequent step, hand layup technique was employed for composite laminate preparation. Finally, for a period of 72 h the laminates were allowed to cure at room temperature.

2.3. FRP wrapping of specimens

The plain concrete specimens after a curing period of 28 days were dried at room temperature after which the surface was cleaned. By means of hand layup process the prepared specimens were confined externally. The schematic representation of preparation of samples is illustrated in Figure 1. Over the cleaned surface of the specimens a layer of epoxy resin was applied. Then, a single layer of fiber sheet impregnated with epoxy was laid over the radial surface. An overlap distance of about 150mm was

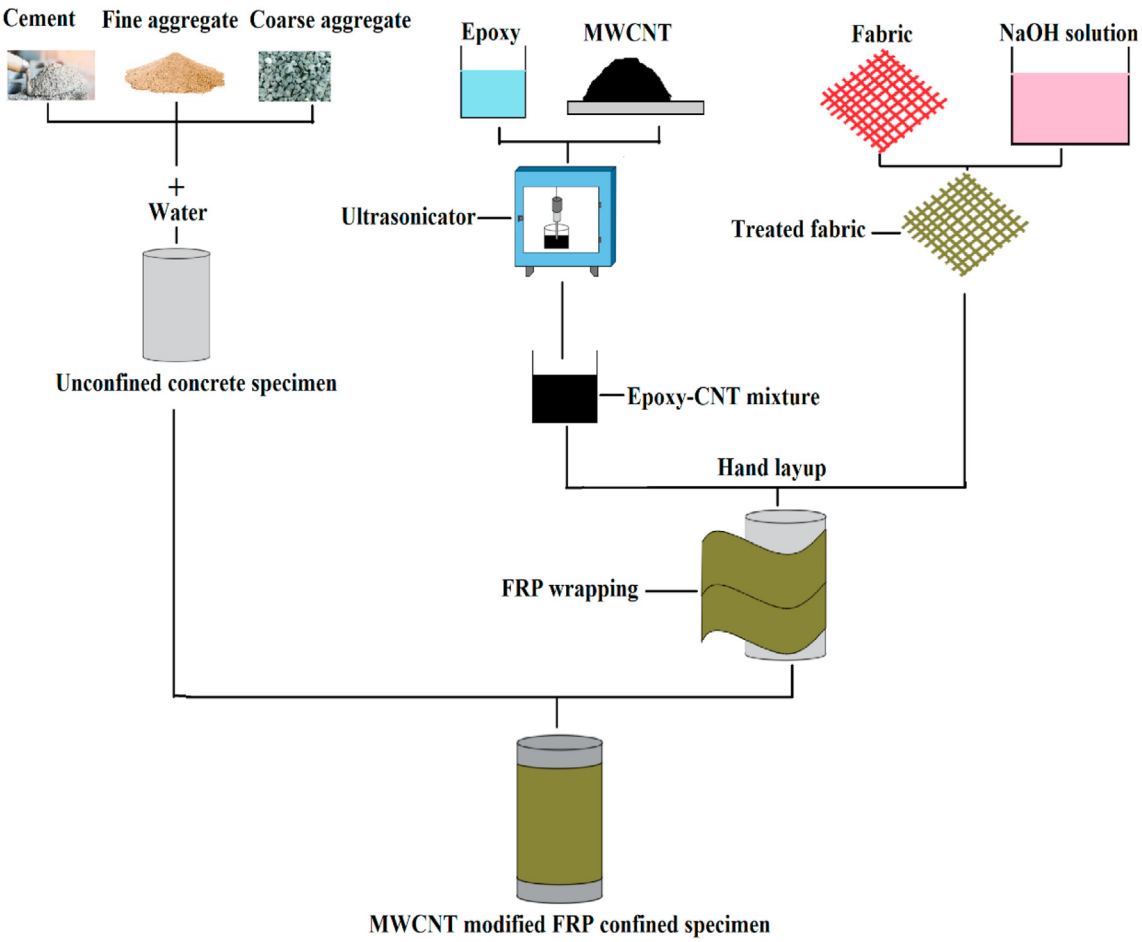

Figure 1. Schematic representation of specimen preparation.

maintained for the successive layers. After the process of wrapping the first fiber sheet, another epoxy resin layer was applied over it and the entrapped air was removed using a roller to provide proper resin impregnation between the layers [36]. Then it was allowed to cure for 24 h and the successive layers were wrapped in the same manner. A proper bonding between the concrete core and external FRP layers was accomplished due to the adhesion characteristics of epoxy resin. Prior to the commencement of the tests, the specimens were allowed to cure for 7 days at room temperature [37].

2.4. Test specimens and test procedure

Cylinders of 300 mm height and 150 mm inside diameter was fixed as base concrete specimens. Figure 2 shows various stages included in specimen preparation. In this work, 60 cylindrical concrete specimens were cast and further tested. Specimens were classified mainly as the control specimens (unconfined specimens), single fiber FRP confined specimens and specimens confined with a hybrid FRP. The test program incorporated numerous hybrid configurations consisting of various inner and outer FRP confinements. The nomenclature used for the test specimens are provided in Table 1. The cast concrete column specimens were tested in axial compression using a 2000kN capacity compression testing machine. 10mm high strength steel plates were kept over the top and bottom sides of the test specimens in order to ensure uniform load application at the concrete core. During the process of testing 0.2 mm/min constant displacement was applied on the specimens. Since a high axial displacement is expected, 1 mm/min constant loading rate was kept. Linear variable differential transducers (LVDTs) with a capacity of 50 mm were used as the instrumentation to record axial strains on the concrete specimens as seen in Figure 3.

3. Results and discussion

3.1. High-resolution transmission electron microscope (HRTEM) analysis of epoxy composites

TEM is the most appropriate methodology adopted to analyze the alignment, morphology distribution and particle size of the filler material [38]. Figure 4 demonstrates the TEM image corresponding to MWCNT-epoxy composites with CNT weight percentage of 0.5%, 1% and 1.5% respectively. In base polymer, the nanoscale dispersion of MWCNT was clearly visible from the TEM images. Presence of nano particle clusters was found in certain spaces even after ultrasonication. The formation of clusters of CNT diminishes the interfacial region which in turn may result in the reduction in chemical and physical bonding between epoxy and MWCNT. Figure 4a depicts the dispersion of 0.5wt. % MWCNT in epoxy. The distribution of CNT is uniform with 1–10 μm average length and 5–10 nm average diameter. Figure 4b portrays the epoxy nanocomposite morphology corresponding to 1wt. % MWCNT and at this wt.% the MWCNT nanoparticles were found to be well distributed within epoxy. The multifarious entanglement of epoxy with MWCNTs can prompt better exchange of applied load which further prevents crack propagation within composites. A combination of MWCNT dispersion and agglomeration was noticed in the TEM images corresponding to 1.5wt. % CNT. The interparticle van der Waals force may be one reason for the development of the agglomerate in the CNTs [39]. The agglomeration was

Figure 2. Various stages involved in specimen preparation.

Table 1. Test specimen details.

Group	Specimen	Core specimen material	CNT %	Number of sisal Layer (Inside)	Number of basalt Layer (Outside)	Total fiber layer	No. of specimens
A	E	Epoxy	0	0	0		3
	EC0.5	Epoxy	0.5	0	0		3
	EC1	Epoxy	1	0	0		3
	EC1.5	Epoxy	1.5	0	0		3
B	EC0S2B0	Epoxy	0	2	0	2	3
	EC0S2B2	Epoxy	0	2	2	4	3
	EC1S2B0	Epoxy	1	2	0	2	3
	EC1S2B2	Epoxy	1	2	2	4	3
C	CS	Concrete	0	0	0		3
	C-EC0S2	Concrete	0	2	0	2	3
	C-EC0S2B1	Concrete	0	2	1	3	3
	C-EC0S2B2	Concrete	0	2	2	4	3
	C-EC0S2B3	Concrete	0	2	3	5	3
D	C-EC0.5S2	Concrete	0.5	2	0	2	3
	C-EC0.5S2B1	Concrete	0.5	2	1	3	3
	C-EC0.5S2B2	Concrete	0.5	2	2	4	3
	C-EC0.5S2B3	Concrete	0.5	2	3	5	3
E	C-EC1S2	Concrete	1	2	0	2	3
	C-EC1S2B1	Concrete	1	2	1	3	3
	C-EC1S2B2	Concrete	1	2	2	4	3
	C-EC1S2B3	Concrete	1	2	3	5	3
F	C-EC1.5S2	Concrete	1.5	2	0	2	3
	C-EC1.5S2B1	Concrete	1.5	2	1	3	3
	C-EC1.5S2B2	Concrete	1.5	2	2	4	3
	C-EC1.5S2B3	Concrete	1.5	2	3	5	3

pronounced at higher CNT content as evidenced from Figure 4c leading to lower interparticle distance and weak mechanical properties.

3.2. Tensile properties of epoxy composites

The tensile properties of epoxy specimens were assessed as per ASTM D3039 using INSTRON 502 Universal testing machine with a crosshead speed of 1 mm/min. The length, width and thickness of the epoxy specimens were 100mm, 10mm, and 3mm respectively. The results are presented in Figure 5 and Table 2 and it was observed that with the addition of MWCNT, there is significant enhancement in tensile properties. With 1wt. % of MWCNT addition, the epoxy composites exhibited a 65% improvement in tensile strength and 41% improvement in Young's modulus with respect to neat epoxy. The huge interfacial area and interaction provides mechanical interlocking between the MWCNT and epoxy chains and thereby results in an anchoring effect. For epoxy hybrid

Figure 3. Compression test setup.

composites with two layers each of basalt and sisal fibers along with 1wt. % of MWCNT, improvement of about 168% in the tensile strength and an 89% enhancement in Young's modulus was noticed. The improvement in tensile strength and modulus may be assigned to the enhanced load bearing capacity of epoxy incorporated with MWCNTs [40]. The initiation of crack commences within the epoxy during the loading process because of its low modulus in comparison with CNT and the mechanical interlocking enables the bridging effect and thus exchange of stresses from the lower to the higher modulus MWCNTs. The interparticle distance between MWCNT diminishes at its higher percentages in epoxy and further it reduces the interfacial interaction between epoxy and MWCNT as well as the fibers. The pronounced agglomeration at 1.5wt. % leads to lower interparticle distance and reduction in the mechanical properties [41].

3.3. Fracture toughness of epoxy composites

Single-edge notched bending (SENB) test was adopted to evaluate the fracture toughness of the composite specimens in a universal testing machine (UTM) with 1 mm/min constant crosshead displacement rate. The stress intensity produced due to the residual stresses is predicted using the linear-elastic fracture toughness of material (K_{IC}) while the measure of energy dissipated during fracture per unit fracture surface area is predicted by plastic-elastic fracture toughness (G_{IC}) [42]. From Table 3 it was observed that with the addition of hybrid fibers there is a prominent improvement in the fracture toughness values compared with neat epoxy resin. At the crack tip, the delamination growth is resisted by the presence of hybrid fibers. The incorporation of MWCNT enhances bridging effect at the crack tip and thus resists crack propagation considerably. For higher weight percentages of MWCNTs, fracture toughness value declines due to the agglomeration of the nanofiller within the epoxy matrix. The improvement in the strength and fracture toughness characteristics can be assigned to uniform dispersion of nanoparticles. Epoxy exhibited an increase in the failure load when filled with MWCNTs [43]. The same was visible in the case of EC0.5 and EC1. These complex polymer chain networks undergo high strain and could reduce the crack propagation providing a large energy release rate. As seen in EC1.5, at higher MWCNT weight percentage, there was a decrease in values of fracture toughness which can be attributed to the aggregation of the nanofiller. It can be concluded that uniform dispersion of nanoparticles has a major significance in performance of a reinforced polymer system.

3.4. Flexural properties of epoxy composites

The flexural tests were carried out as per ASTM D790 in a 3-point bending mode using UTM at 1.25 mm/min crosshead speed. The flexural modulus and strength of the various composites were assessed and reported in Figure 6. For the neat epoxy resin, the flexural strength was found to be 100MPa whereas that of the composite with 1wt % MWCNT manifested 160 MPa. The presence of MWCNTs enables the epoxy chains to resist elevated bending loads due to the anchoring effect [44]. The maximum increase in flexural strength was exhibited with 1wt. % addition of MWCNT. For epoxy hybrid composites with two layers of basalt and sisal fibers each, and 1wt. % of MWCNT, there was an increment of about 120% in the flexural strength. But there was a decline in flexural properties beyond 1wt. % addition of MWCNT due to the reduction in the free volume space leading to the impeded mobility of epoxy chains.

3.5. Dynamic mechanical analysis (DMA) of epoxy composites

DMA is an excellent technique to estimate the interfacial interaction between the viscoelastic type of matrix material and the reinforcements in composite systems [45]. Since the response is recorded in terms of storage modulus, loss modulus and damping factor, inferences may be drawn on the suitability of such materials in dynamic loading situations. The analysis was carried out on epoxy nanocomposites rectangular

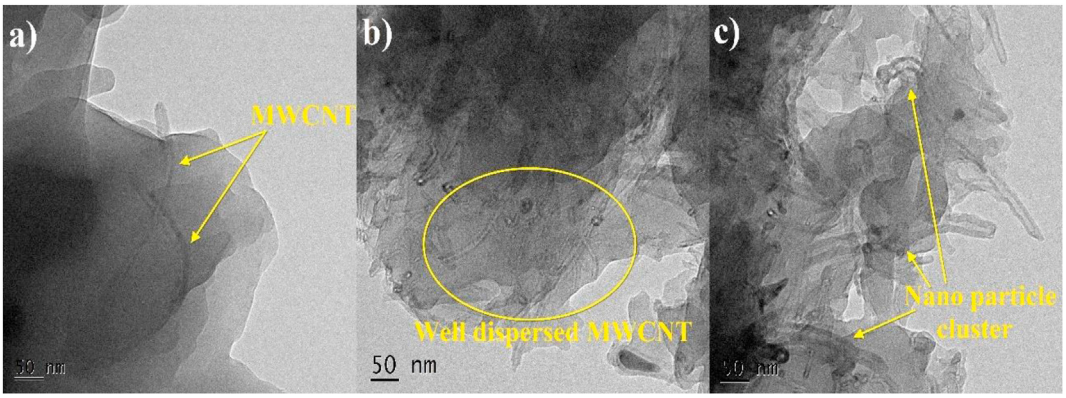

Figure 4. TEM images of a) EC0.5 b) EC1 c) EC1.5 nano composites.

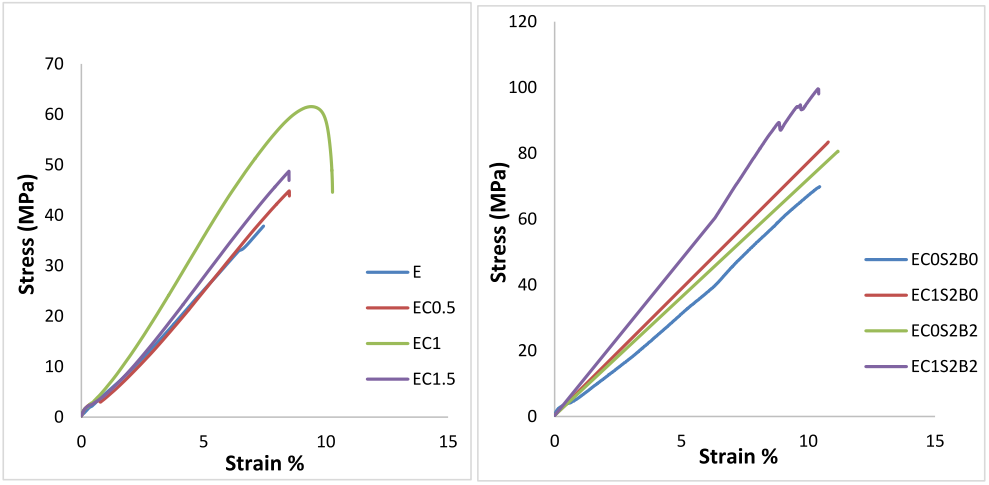

(a) Epoxy Composite (b) Hybrid Composite

Figure 5. Tensile stress-strain curve for epoxy and hybrid composites.

Table 2. Tensile properties of epoxy and hybrid composites.

Sample	Tensile strength (MPa)	Young's modulus (GPa)	Elongation (%)
E	37 ± 0.8	1.82 ± 0.02	7.3 ± 0.4
EC0.5	44 ± 0.8	1.98 ± 0.03	8.5 ± 0.2
EC1	61 ± 0.1	2.56 ± 0.02	10.2 ± 0.1
EC1.5	48 ± 0.7	2.20 ± 0.04	8.4 ± 0.1
EC0S2B0	69 ± 0.8	2.88 ± 0.03	10.2 ± 0.2
EC0S2B2	72 ± 1.8	2.96 ± 0.80	10.7 ± 0.8
EC1S2B0	83 ± 2.0	3.18 ± 0.80	11.5 ± 0.6
EC1S2B2	99 ± 2.1	3.44 ± 0.90	10.3 ± 0.9

Table 3. Fracture toughness properties of epoxy and hybrid composites.

Sample	K_{IC} (MPa.m$^{1/2}$)	G_{IC} (kJ/m^2)
E	1.7 ± 0.2	1.5 ± 0.4
EC0.5	3.0 ± 0.1	4.5 ± 0.3
EC1	4.0 ± 0.2	6.2 ± 0.4
EC1.5	3.4 ± 0.3	5.2 ± 0.1
EC0S2B0	3.4 ± 0.1	4.0 ± 0.1
EC0S2B2	4.5 ± 0.8	6.8 ± 0.6
EC1S2B0	3.8 ± 0.7	4.5 ± 0.6
EC1S2B2	5.6 ± 0.8	9.2 ± 0.8

samples of 2mm thickness using PerkinElmer DMA800 in three-point bending mode in the temperature range of 25–160 °C at a heating rate of 5 °C/min at a fixed frequency of 1 Hz as per ASTM D 5023.

Figure 7 delineates the variation of storage modulus with temperature of neat epoxy and nanocomposites. Elastic response of the material can be estimated from storage modulus and it is evident that the composite with 1wt. % loading of MWCNT exhibits exemplary storage modulus up to 70 °C. The rigidity and thereby the binding capability of nano modified epoxy can be considered to be superior as the storage modulus in the three-point bending mode can be taken as a relative measure of the flexural strength of the composite. Further, the dip in storage modulus from a plateau region to a steep slope region with a characteristic shoulder occurs at a higher temperature in the case of EC1. The sharp drop in storage modulus occurs at the glass transition temperature (Tg) of epoxy is due to the segmental mobility of polymer chains. The mobility of the polymer chains is hindered by the dispersion of nanofiller elevating the mechanical properties of the nano modified epoxy.

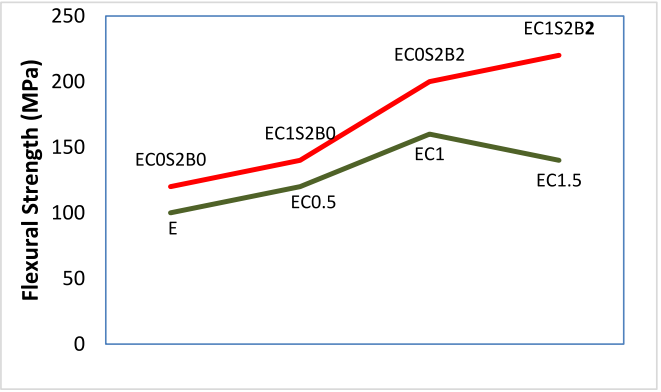

Figure 6. Flexural strength of epoxy hybrid composites.

The loss modulus variation of the samples with temperature is illustrated in Figure 8 and the peak value is observable at the glass transition temperature, beyond which it drops. The higher loss modulus presented by EC1 is due to the superlative energy dissipation characteristics and better interfacial adhesion prevalent between the MWCNT and epoxy macromolecules. Furthermore, a shift in the glass transition towards the higher temperature was manifested with increase in MWCNT content in epoxy.

The variation of mechanical damping factor (tan delta) with temperature for epoxy and nanocomposites is presented in Figure 9. The shortening and broadening of the tan delta peak of EC1 is a testimony of the immobilization of the long chain polymer molecules as they are anchored onto the MWCNTs. The broadening of the peak aids the energy absorption during dynamic loading. The Tg value obtained from the tan delta peak is highest for EC1, followed by EC0.5. The superior performance of the epoxy nanocomposites in dynamic loading scenarios can thus be established by the dynamic mechanical analysis studies.

3.6. Confinement effect of FRP wrapping on concrete

3.6.1. Effect of epoxy modification by MWCNT

The specimens in Group C, D, E and F were used to investigate the confinement effect due to the percentage variation of CNT on the ductility and load-carrying capacity of cylinders confined with different types of FRP jackets. Epoxy-MWCNT nanocomposites containing 0.5, 1 and 1.5wt. % of CNT were prepared and applied in between the fiber layers as adhesive.

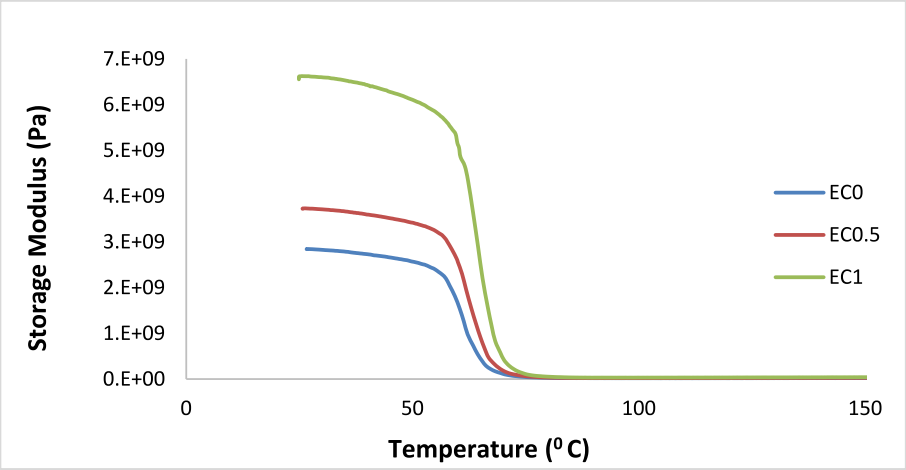

Figure 7. Variation of storage modulus with temperature for epoxy and nanocomposites.

3.6.1.1. Axial compressive behavior. In Table 4 the results of axial compression test for specimens confined with different FRP's for different percentage variation of CNT are presented. f'_{co} indicates the unconfined concrete strength and f'_{cc} as that of the FRP confined concrete. In the case of FRP wrapped concrete the confinement effectiveness is represented by f'_{cc}/f'_{co}. The axial strain for unconfined and FRP strengthened specimens were represented by ε_{co} and ε_{cc} respectively. From the test results a significant improvement in load carrying capacity by the jacketing of plain concrete cylinders with FRP was evident.

The greatest improvement in axial load carrying capacity was observed for 1wt. % of MWCNT incorporated FRP wrapped specimens followed by 1.5wt. % as presented in Figure 10. The confinement effectiveness for 1.5,1,0.5 wt.% of MWCNT modified epoxy wrapped specimens and neat epoxy wrapped specimens are 1.71, 1.90, 1.62 and 1.45 respectively with respect to plain concrete for 5 layers of hybrid wrapping. The effect of confinement offered by the MWCNT incorporation was the major reason for improved axial load carrying capacity. There is also a pronounced improvement in the load carrying capacity of hybrid sisal and basalt fiber composite wrapped concrete cylinders. Individual sisal FRP confinement exhibited an increase in load carrying capacity significantly but when compared, hybrid composite jacketing performed better. This is due to the synergetic effect offered by the hybrid fibers to the structure's improved load bearing capacity [11].

3.6.1.2. Stress-strain response. The axial compressive stress behavior of control and MWCNT incorporated FRP jacketed cylinders is delineated in Figure 11. While the plain concrete specimens exhibited a single linear regime in the stress-strain curve, the FRP confined specimens manifested different regimes [1]. The initial region of the curve exhibited almost a similar behavior as that of unconfined specimens. In the first region, due to insignificant lateral deformation of core, the effect of FRP jacketing is not appreciable. A transition zone is developed where the micro-cracks are observed, when applied stress reaches the ultimate compressive strength. Eventually, the effect of confinement was activated in the next stage of the stress-strain curve on reaching the peak compressive strength. Beyond that, with reduced slope a linear trend was observed. Thus, the last two stages of the curve exhibited superior confinement effect due to the presence of MWCNT in the epoxy matrix. These two stages usually govern the ultimate properties of the concrete and the MWCNT incorporated FRP. Control specimens exhibit failures at the end of the initial stage itself due to its brittle nature [46]. On the contrary, MWCNT incorporated FRP confined specimens after yielding shows ductile mode of failure. Further studies were carried out for different weight percentages of MWCNT incorporated FRP jacketing and upon analysis of test results it was clear that 1% of MWCNT incorporated FRP wrapped specimens exhibited better ductile and yielding properties. Similar results were reported in previous study involved [6]. An enhancement in axial compressive strength and strain was observed with increase in FRP layers as an indication of a linear relation between number of FRP layers. Ispir et al. [11] studied the influence of different fibers in hybrid fiber system and inferred that inner and outer FRP layers rupture simultaneously and the one with low elongation capacity tends to rupture first. The general failure patterns exhibited by confined and unconfined specimens are shown in Figure 12. The chance for catastrophic failure is reduced, proving its potential application in earthquake prone areas [2].

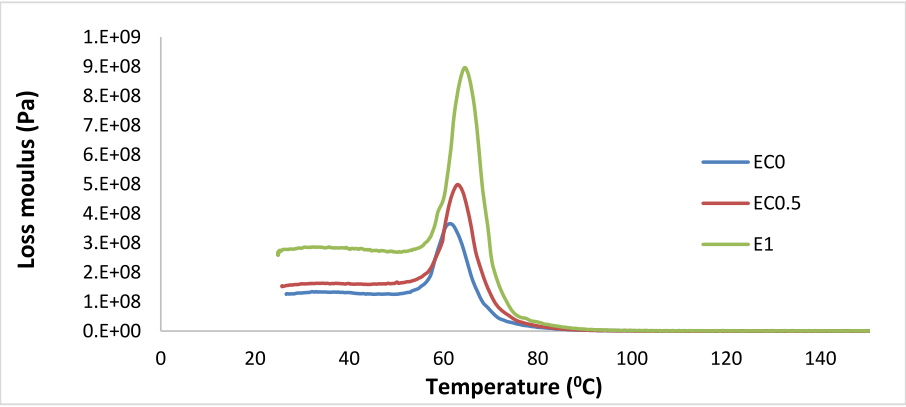

Figure 8. The variation of loss modulus with temperature for epoxy and nanocomposites.

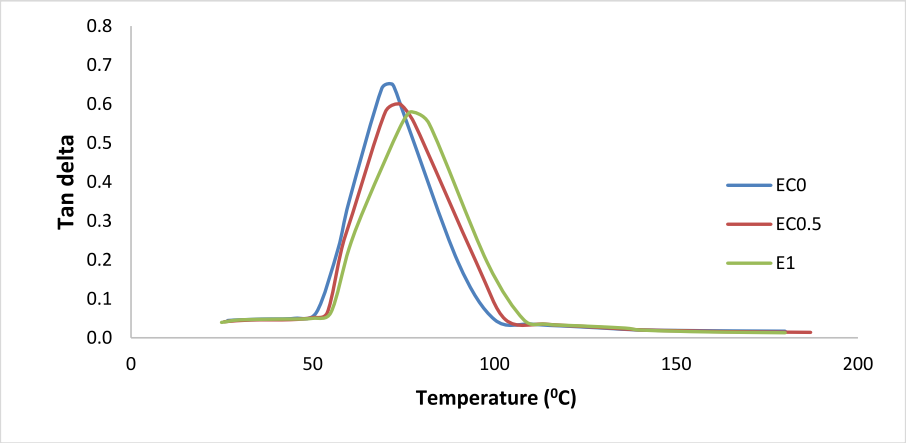

Figure 9. Variation of mechanical damping factor (Tan delta) with temperature for epoxy and nanocomposites.

Table 4. Compression test results of CNT modified FRP confined specimens.

Sl No	Specimen	Compressive strength (MPa) (f'_{cc} or f'_{co})	Strength enhancement %	confinement effectiveness f'_{cc}/f'_{co}	Axial compressive strain (ε_{cc} or ε_{co})	Modulus of Elasticity (GPa)
1	CS	14.29	-		0.36	9.40
2	C-EC0S2	16.89	18.18	1.18	1.06	10.10
3	C-EC0S2B1	18.84	31.82	1.32	1.23	10.20
4	C-EC0S2B2	20.79	45.45	1.45	1.41	10.40
5	C-EC0S2B3	23.39	63.64	1.64	1.45	10.60
6	C-EC0.5S2	18.19	27.27	1.27	1.32	10.20
7	C-EC0.5S2B1	21.44	50.00	1.50	1.53	10.60
8	C-EC0.5S2B2	25.33	77.27	1.77	1.54	10.90
9	C-EC0.5S2B3	27.93	95.45	1.95	1.62	11.20
10	C-EC1S2	20.79	45.45	1.45	1.50	10.30
11	C-EC1S2B1	25.33	77.27	1.77	1.56	10.80
12	C-EC1S2B2	27.28	90.91	1.91	1.64	11.10
13	C-EC1S2B3	30.53	113.64	2.14	1.90	11.60
14	C-EC1.5S2	18.84	31.82	1.32	1.45	10.20
15	C-EC1.5S2B1	20.79	45.45	1.45	1.41	10.30
16	C-EC1.5S2B2	25.98	81.82	1.82	1.48	10.90
17	C-EC1.5S2B3	28.58	100.00	2.00	1.71	11.40

3.6.1.3. Ductile behavior and energy absorption. It is generally recommended that the structure may undergo considerable deformation in order to avoid catastrophic failure. The members with high energy absorption rate, coupled with ductile behavior helps in providing sufficient warnings before failure. An increase in efficiency of confinement leads to increased ductility which in turn elevates the energy absorption

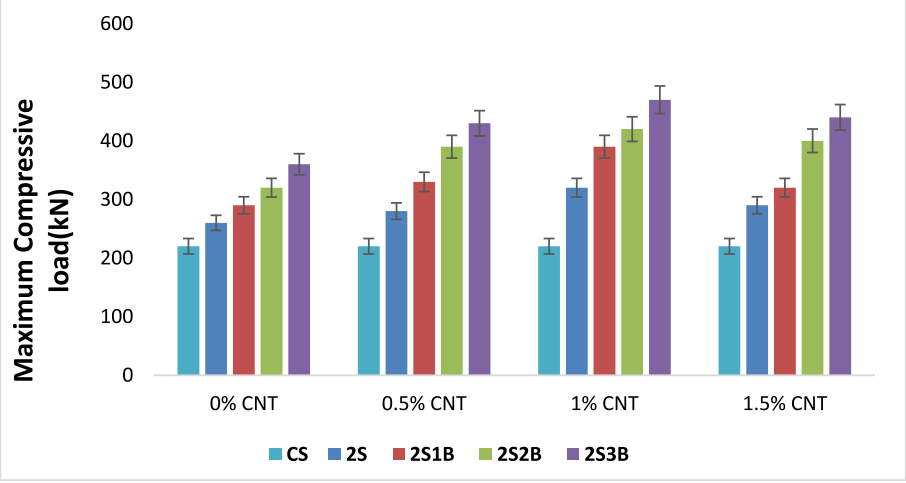

Figure 10. Maximum compressive load of specimens.

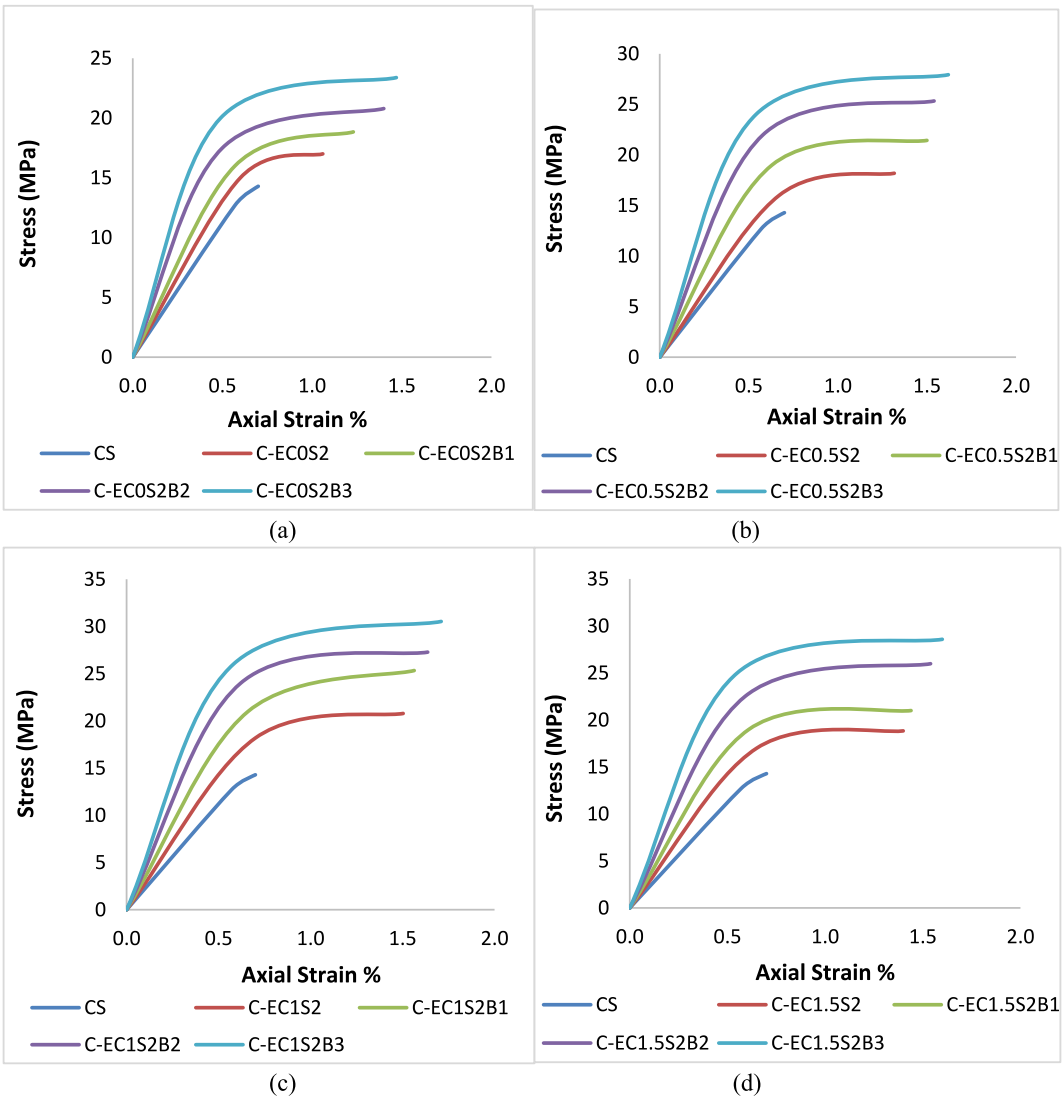

Figure 11. Axial stress-strain curves of specimens with a) 0wt. % b) 0.5wt. % o c) 1wt. % and d) 1.5wt. % of CNT.

Figure 12. Failure pattern (a) Plain concrete (Control Cylinder) and (b) confined cylinder (C-C1S2B3).

Table 5. Energy ductility index of different layer of CNT modified FRP confined specimens.

Sl No	Specimen	Energy absorbed (MPa)	Energy ductility index
1	CS	5.37	1
2	C-EC0S2	11.86	2.07
3	C-EC0S2B1	16.05	2.83
4	C-EC0S2B2	21.60	3.85
5	C-EC0S2B3	26.15	4.75
6	C-EC0.5S2	16.41	2.98
7	C-EC0.5S2B1	23.57	4.32
8	C-EC0.5S2B2	29.10	5.35
9	C-EC0.5S2B3	34.52	6.36
10	C-EC1S2	22.02	4.03
11	C-EC1S2B1	27.85	5.11
12	C-EC1S2B2	33.50	6.17
13	C-EC1S2B3	39.48	7.29
14	C-EC1.5S2	19.14	3.50
15	C-EC1.5S2B1	22.66	3.96
16	C-EC1.5S2B2	28.21	5.17
17	C-EC1.5S2B3	37.95	7.01

Table 6. Compression test results of different FRP systems.

Sl No	Specimen	FRP	Compressive strength (MPa) (f_{cc} or f_{co})	Strength enhancement %	Confinement effectiveness f_{cc}/f_{co}	Axial compressive strain (ε_{cc} or ε_{co})	Modulus of Elasticity (GPa)
1	CS		14.29	-		0.36	9.40
2	C-EC1S2	SFRP	20.79	45.45	1.45	1.50	10.30
3	C-EC1B2	BSRP	24.04	68.18	1.68	1.56	10.80
4	C-EC1Ca1	CFRP	26.63	86.36	1.86	1.58	10.94
5	C-EC1S2B2	HSBFRP	27.28	90.91	1.91	1.64	11.10

without catastrophic failure. The ductility index is used as the measure of the ductility which is defined as the ratio of fracture energy of FRP confined to plain concrete [47].

The ductility and energy absorption values for different confined specimens are given in Table 5. It is evident that FRP confinement increases the ductility characteristics to a greater extent. Due to monolithic compressive behavior, the specimen C-EC1S2B3 showed an energy absorption value of 39.48 MPa, showing an increase of about 87% and ductility index value of 7.35 relative to the control specimen. It was noticed that CNT modified FRP confinement exhibited an increase from 68% to 87% in their energy absorption values relative to control specimen and in non-CNT incorporated FRP confinement the increased energy absorption is due to the contribution from FRP confinement wraps. Conclusions were made that apart from compressive strength improvement, FRP wrapping improved the fracture energy as well as ductility of the confined concrete specimens [48].

3.6.2. *Effect of different types of fibers*

The specimens with different types of FRP confinement were adopted to analyze the influence of different fiber systems on the ductility and load-carrying capacity of confined specimens with FRP jackets. The various specimens considered are sisal fiber reinforced polymer (SFRP) wrapped with two layers of FRP confinement, basalt fiber reinforced polymer (BFRP) wrapped specimen with two layers of FRP confinement, hybrid sisal-basalt fiber reinforced polymer (HSBFRP) wrapped specimen with four layers of FRP confinement with two layers sisal and basalt fiber layers each, carbon fiber reinforced polymer (CFRP) wrapped specimen with single layer of carbon FRP confinement.

3.6.2.1. Axial compressive behavior. The results of axial compression tests conducted on various column specimens jacketed with different types of fiber systems are presented in Table 6. The highest load carrying capacity was exhibited by HSBFRP specimens followed by a single layer of CFRP wrapped specimen. The confining pressure effect offered by modified FRP around the unconfined specimens was found to be the reason for enhanced axial load carrying capacity [37]. From the listed FRP types, both CFRP and HSBFRP composite jacketing exhibited better performance in terms of axial load carrying capacity. Even the individual BFRP and SFRP confinement exhibited satisfying property improvement. HSBFRP composite wrapping performed better when compared with individual basalt, sisal and carbon confinement. The strength enhancement is due to the synergetic impact of both the fibers in improving the load bearing capacity of the specimens. A significant improvement in ductile performance was evidenced in all specimens with FRP wraps.

3.6.2.2. Stress- strain response. The axial compressive stress versus axial strain observed for specimens jacketed with different fiber systems is presented in Figure 13. The stress-strain curve exhibited different regimes in the case of confined specimens. When control specimens are considered, they tend to fail during the end of the initial stage due to the brittle nature of control specimens. FRP confined specimens exhibited ductile nature i.e., failure occurs after FRP yielding [6]. The addition of natural fiber has exhibited sensible enhancement in the ductile nature of confined specimens. From Table 7 it was clear that when compared, the structural properties particularly ductile behavior was commendable

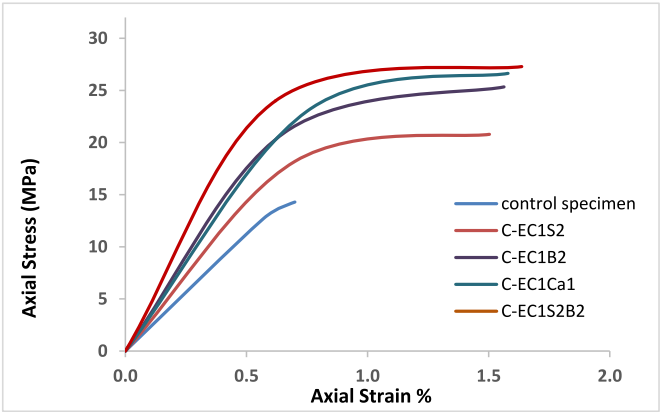

Figure 13. Axial stress-strain curves of specimens confined with different FRP systems.

when confined with HSBFRP. The stress-strain plot for HSBFRP confined specimens exhibited similar trends as that of individual sisal and basalt FRP confined specimens. It may be noted that during first stage HSBFRP confinement has less impact due to the insignificant deformations concentrating in the concrete core. Once the ultimate compressive strength is reached in case of unconfined columns, a transitional zone may be noted along with development of numerous micro-cracks. While in case of confined specimens at this stage the confinement effect offered by HSBFRP laminate will be completely activated. The second stage was found to be dominated by the combined properties offered by FRP and concrete. It was noticed that the inner fiber sheet possesses lower elongation properties and they tend to rupture first and the outer basalt layer survives for a long period in case of hybrid systems. This may be due to the dominance offered by basalt FRP as it could contain greater rupture strain. Similar studies were conducted by Rousakis [13] on the performance of hybrid FRP systems. Major observations were made that during the failure process a significant drop in load carrying capacity was noticed after the inner sisal sheets being fractured and energy was released but similar energy was found to be absorbed by the fiber sheets and further enables the specimens to have a ductile failure. It was clear that HSBFRP and CFRP wrapped specimens survived more in the second and final stage exhibiting their better ductile and yielding properties. Thus, reducing the probability of catastrophic failure [46].

3.6.2.3. Ductile behavior and energy absorption. The energy absorption and ductility index values corresponding to different FRP jacketed

Table 7. Energy ductility index of concrete strengthened with different FRP systems.

Sl No	Specimen	Energy absorbed (MPa)	Energy ductility index
1	CS	5.37	1
2	C-EC1S2	22.02	4.10
3	C-EC1B2	27.85	5.18
4	C-EC1Ca1	31.23	5.81
5	C-EC1S2B2	33.50	6.24

specimens are given in Table 7. A significant enhancement in fracture energy was observed in HSBFRP specimens compared to control specimens along with enhancement the ductile behavior and energy absorption property. The control specimen exhibited a moderate energy absorption value and was evident that FRP confinement ramps up the ductility characteristics of the unconfined cylinders [3]. The HSBFRP specimens exhibited a monolithic compressive behavior and recorded an energy absorption value of 33.50 MPa, with an increase of about 523% with respect to the unconfined ones, and ductility index value of 6.24 when compared. At the same time the CFRP specimen recorded an energy absorption value of 31.23 MPa, showing increases of about 481% and ductility index value of 5.81. This enhancement was found to be due to the FRP modifications. It was noticed that sisal FRP confinement exhibited an increase in their energy absorption when compared with that of control specimens by 310% and the impact of the same was visible in HSBFRP confined specimens too. Thus, conclusions may be made that HSBFRP composite wrapping could improve the fracture energy and ductility property of confined concrete columns and thereby exhibiting an excellent solution for systems lacking internal reinforcement [47].

4. Conclusions

The systematic study on the efficacy of MWCNT modified epoxy with hybrid fibers as a noteworthy option for the strengthening of concrete structures is reported in the present paper. From the research outcomes obtained, the following conclusions were drawn.

- The load bearing ability in the axial direction of the structure could be remarkably improved by FRP wrapping as evidenced from the compression test results. Additionally, a pronounced improvement in ductility characteristics, fracture energy and axial strain could also be accomplished.
- The optimum MWCNT content in epoxy was found to be 1wt. % for maximum improvement in mechanical properties for nano and multiscale composites. The MWCNT content and its uniform dispersion governs the enhanced properties. Beyond 1wt. % the tensile properties diminished due to agglomeration of nanofillers.
- Significant improvement in flexural properties was seen with MWCNT content in both epoxy and epoxy-MWCNT-fiber multiscale composites. With an enhancement of 60% for epoxy composites and 120% for epoxy fiber multiscale composites containing 1wt. % of MWCNT
- The hybrid confinement is powerful in working on the straining capacity and compressive strength of both FRP and MWCNT modified FRP composites. The enhancement in strength and ultimate strain are found to be influenced by the count of FRP layers and percentage of MWCNT modification.
- The strain behavior of individual FRP systems dominates the ultimate stress-strain behavior of confined specimens. Beyond the peak strength of concrete until ultimate state is achieved, when the inner FRP layers ruptures the required resistance is provided by the outer FRP layers against lateral expansion of the core.
- In confined concrete the ductility index and fracture energy were fundamentally improved with hybrid confinement and they significantly varied with the quantity of FRP layers and MWCNT modification.
- The outer FRP jackets assisted in resisting the externally applied loads after a significant period of ultimate loading and thereby avoiding catastrophic failure to an extent.

Hence based on the test results it was concluded that the epoxy modified with MWCNT is a good option for the repair and retrofitting of concrete structures. The low strength of natural FRP confinement compared to artificial FRP is taken care of by this epoxy modification. Thus, the present system can be utilized in seismic prone areas where greater ductility and strength properties are required.

Declarations

Author contribution statement

Lakshmi Joseph: Conceived and designed the experiments; Performed the experiments; Analyzed and interpreted the data; Contributed reagents, materials, analysis tools or data; Wrote the paper.

P. Sarath Kumar & B. D. S. Deeraj: Performed the experiments.

K. Joseph: Analyzed and interpreted the data.

Karingamanna Jayanarayanan & Mini K.M: Conceived and designed the experiments; Analyzed and interpreted the data; Contributed reagents, materials, analysis tools or data; Wrote the paper.

Funding statement

This research did not receive any specific grant from funding agencies in the public, commercial, or not-for-profit sectors.

Data availability statement

Data included in article/supp. material/referenced in article.

Declaration of interest's statement

The authors declare no conflict of interest.

Additional information

No additional information is available for this paper.

References

[1] A. Padanattil, J. Karingamanna, K.M. Mini, Novel hybrid composites based on glass and sisal fiber for retrofitting of reinforced concrete structures, Construct. Build. Mater. 133 (2017) 146–153.
[2] N. Wahab, P. Srinophakun, Q. Hussain, P. Chaimahawan, Performance of concrete confined with a jute–polyester hybrid Fiber reinforced polymer composite: a novel strengthening technique, Fibers 7 (8) (2019) 72.
[3] Shamsher Bahadur Singh, Analysis and Design of FRP Reinforced Concrete Structures, second ed., Tata McGraw-Hill Publishing Company Limited, New Delhi, 2013.
[4] L. Ghalieh, E. Awwad, G. Saad, H. Khatib, M. Mabsout, Concrete columns wrapped with hemp fiber reinforced polymer–an experimental study, Procedia Eng. 200 (2017) 440–447.
[5] S. Siriluk, Q. Hussain, W. Rattanapitikorn, A. Pimanmas, Behaviors of RC deep beams strengthened in shear using hemp fiber reinforced polymer composites, Int. J. 15 (47) (2018) 89–94.
[6] T. Sen, A. Paul, Confining concrete with sisal and jute FRP as alternatives for CFRP and GFRP, International Journal of Sustainable Built Environment 4 (2) (2015) 248–264.
[7] T.M. Gowda, A.C.B. Naidu, R. Chhaya, Some mechanical properties of untreated jute fabric-reinforced polyester composites, Compos. Appl. Sci. Manuf. 30 (3) (1999) 277–284.
[8] P. Taghia, S.A. Bakar, Mechanical behavior of confined reinforced concrete-CFRP short column-based on finite element analysis, World Appl. Sci. J. 24 (7) (2013) 960–970.
[9] H.S. Kim, Y.S. Shin, Flexural behavior of reinforced concrete (RC) beams retrofitted with hybrid fiber reinforced polymers (FRPs) under sustaining loads, Compos. Struct. 93 (2) (2011) 802–811.
[10] M. Ramesh, K. Palanikumar, K.H. Reddy, Mechanical property evaluation of sisal–jute–glass fiber reinforced polyester composites, Compos. B Eng. 48 (2013) 1–9.
[11] M. Ispir, K.D. Dalgic, A. Ilki, Hybrid confinement of concrete through use of low and high rupture strain FRP, Compos. B Eng. 153 (2018) 243–255.
[12] B.V. Ramnath, S.J. Kokan, R.N. Raja, R. Sathyanarayanan, C. Elanchezhian, A.R. Prasad, V.M. Manickavasagam, Evaluation of mechanical properties of abaca–jute–glass fibre reinforced epoxy composite, Mater. Des. 51 (2013) 357–366.
[13] T.C. Rousakis, K.B. Kouravelou, T.K. Karachalios, Effects of carbon nanotube enrichment of epoxy resins on hybrid FRP–FR confinement of concrete, Compos. B Eng. 57 (2014) 210–218.
[14] T.C. Rousakis, Inherent seismic resilience of RC columns externally confined with nonbonded composite ropes, Compos. B Eng. 135 (2018) 142–148.
[15] F. Faleschini, M.A. Zanini, L. Hofer, C. Pellegrino, Experimental behavior of reinforced concrete columns confined with carbon-FRCM composites, Construct. Build. Mater. 243 (2020), 118296.

[16] F. Longo, A. Cascardi, P. Lassandro, M.A. Aiello, A new Fabric Reinforced Geopolymer Mortar (FRGM) with mechanical and energy benefits, Fibers 8 (8) (2020) 49.
[17] T. Trapko, The effect of high temperature on the performance of CFRP and FRCM confined concrete elements, Compos. B Eng. 54 (2013) 138–145.
[18] M.E. Islam, T.H. Mahdi, M.V. Hosur, S. Jeelani, Characterization of carbon fiber reinforced epoxy composites modified with nanoclay and carbon nanotubes, Procedia Eng. 105 (2015) 821–828.
[19] H. Ishida, D.A. Zimmerman, The development of an epoxy resin system for the injection molding of long-fiber epoxy composties, Polym. Compos. 15 (2) (1994) 93–100.
[20] G. Vaganov, V. Yudin, J. Vuorinen, E. Molchanov, Influence of multiwalled carbon nanotubes on the processing behavior of epoxy powder compositions and on the mechanical properties of their fiber reinforced composites, Polym. Compos. 37 (8) (2016) 2377–2383.
[21] T. McNally, P. Pötschke, P. Halley, M. Murphy, D. Martin, S.E. Bell, J.P. Quinn, Polyethylene multiwalled carbon nanotube composites, Polymer 46 (19) (2005) 8222–8232.
[22] J. Ervina, M. Mariatti, S. Hamdan, Effect of filler loading on the tensile properties of multi-walled carbon nanotube and graphene nanopowder filled epoxy composites, Procedia Chem. 19 (2016) 897–905.
[23] A. Godara, L. Mezzo, F. Luizi, A. Warrier, S.V. Lomov, A.W. Van Vuure, I. Verpoest, Influence of carbon nanotube reinforcement on the processing and the mechanical behavior of carbon fiber/epoxy composites, Carbon 47 (12) (2009) 2914–2923.
[24] M.K. Pitchan, S. Bhowmik, M. Balachandran, M. Abraham, Effect of surface functionalization on mechanical properties and decomposition kinetics of high performance polyetherimide/MWCNT nano composites, Compos. Appl. Sci. Manuf. 90 (2016) 147–160.
[25] P.S. Kumar, K. Jayanarayanan, B.D.S. Deeraj, K. Joseph, M. Balachandran, Synergistic effect of carbon fabric and multiwalled carbon nanotubes on the fracture, wear and dynamic load response of epoxy-based multiscale composites, Polym. Bull. (2021) 1–22.
[26] P.S. Kumar, K. Jayanarayanan, M. Balachandran, Thermal and mechanical behavior of functionalized MWCNT reinforced epoxy carbon fabric composites, Mater. Today Proc. 24 (2020) 1157–1166.
[27] Q. Hussain, W. Rattanapitikon, A. Pimanmas, Axial load behavior of circular and square concrete columns confined with sprayed fiber-reinforced polymer composites, Polym. Compos. 37 (8) (2016) 2557–2567.
[28] Q. Hussain, A. Ruangrassamee, S. Tangtermsirikul, P. Joyklad, A.C. Wijeyewickrema, Low-cost fiber rope reinforced polymer (FRRP) confinement of square columns with different corner radii, Buildings 11 (8) (2021) 355.
[29] P.S. Theint, A. Ruangrassamee, Q. Hussain, Strengthening of shear-critical RC columns by high-strength steel-rod collars, Eng. J. 24 (3) (2020) 107–128.
[30] P. Joyklad, S. Suparp, Q. Hussain, Flexural response of JFRP and BFRP strengthened RC beams, Int. J. Eng. Technol. 11 (3) (2019).
[31] A. Pimanmas, Q. Hussain, A. Panyasirikhunawut, W. Rattanapitikon, Axial strength and deformability of concrete confined with natural fibre-reinforced polymers, Mag. Concr. Res. 71 (2) (2019) 55–70.
[32] IS 12269: 2013, Ordinary Portland Cement, 53 Grade –Specification (First revision).
[33] IS 10262-2009, Guidelines for Concrete Mix Design Proportioning.
[34] W. Ouarhim, N. Zari, R. Bouhfid, Mechanical performance of natural fibers–based thermosetting composites, in: Mechanical and Physical Testing of Biocomposites, Fibre-Reinforced Composites and Hybrid Composites, Woodhead Publishing, 2019, pp. 43–60.
[35] M. Tehrani, A.Y. Boroujeni, T.B. Hartman, T.P. Haugh, S.W. Case, M.S. Al-Haik, Mechanical characterization and impact damage assessment of a woven carbon fiber reinforced carbon nanotube–epoxy composite, Compos. Sci. Technol. 75 (2013) 42–48.
[36] S.T. Smith, S.J. Kim, H. Zhang, Behavior and effectiveness of FRP wrap in the confinement of large concrete cylinders, J. Compos. Construct. 14 (5) (2010) 573–582.
[37] R. Benzaid, H. Mesbah, N.E. Chikh, FRP-confined concrete cylinders: axial compression experiments and strength model, J. Reinforc. Plast. Compos. 29 (16) (2010) 2469–2488.
[38] N. Rasana, K. Jayanarayanan, Experimental and micromechanical modeling of fracture toughness: MWCNT-reinforced polypropylene/glass fiber hybrid composites, J. Thermoplast. Compos. Mater. 32 (8) (2019) 1031–1055.
[39] Y. Xue, W. Wu, O. Jacobs, B. Schädel, Tribological behavior of UHMWPE/HDPE blends reinforced with multi-wall carbon nanotubes, Polym. Test. 25 (2) (2006) 221–229.
[40] Z.A. Ghaleb, M. Mariatti, Z.M. Ariff, Synergy effects of graphene and multiwalled carbon nanotubes hybrid system on properties of epoxy nanocomposites, J. Reinforc. Plast. Compos. 36 (9) (2017) 685–695.
[41] J. Zhang, R. Zhuang, J. Liu, E. Mäder, G. Heinrich, S. Gao, Functional interphases with multi-walled carbon nanotubes in glass fibre/epoxy composites, Carbon 48 (8) (2010) 2273–2281.
[42] K.W. Kim, D.K. Kim, B.S. Kim, K.H. An, S.J. Park, K.Y. Rhee, B.J. Kim, Cure behaviors and mechanical properties of carbon fiber-reinforced nylon6/epoxy blended matrix composites, Compos. B Eng. 112 (2017) 15–21.
[43] A.O. Alhareb, H.M. Akil, Z.A. Ahmad, Impact strength, fracture toughness and hardness improvement of PMMA denture base through addition of nitrile rubber/ceramic fillers, The Saudi Journal for Dental Research 8 (1-2) (2017) 26–34.
[44] M.T. Kim, K.Y. Rhee, J.H. Lee, D. Hui, A.K. Lau, Property enhancement of a carbon fiber/epoxy composite by using carbon nanotubes, Compos. B Eng. 42 (5) (2011) 1257–1261.
[45] K. Jayanarayanan, N. Rasana, R.K. Mishra, Dynamic mechanical thermal analysis of polymer nanocomposites, in: Thermal and Rheological Measurement Techniques for Nanomaterials Characterization, Elsevier, 2017, pp. 123–157.
[46] D. Choi, S. Vachirapanyakun, S.Y. Kim, S.S. Ha, Ductile fiber wrapping for seismic retrofit of reinforced concrete columns, Journal of Asian Concrete Federation 1 (1) (2015) 37–46.
[47] L. Yan, Plain concrete cylinders and beams externally strengthened with natural flax fabric reinforced epoxy composites, Mater. Struct. 49 (6) (2016) 2083–2095.
[48] S.A. Dadvar, D. Mostofinejad, H. Bahmani, Strengthening of RC columns by ultra-high performance fiber reinforced concrete (UHPFRC) jacketing, Construct. Build. Mater. 235 (2020), 117485.